NASA Technical Memorandum 104461

Exponential Integration Algorithms Applied to Viscoplasticity

A.D. Freed
Lewis Research Center
Cleveland, Ohio

and

K.P. Walker
Engineering Science Software, Inc.
Smithfield, Rhode Island

Prepared for the
Third International Conference on Computational Plasticity
Fundamentals and Applications (COMPLAS III)
sponsored by the Centro Internacional de Métodos Numéricos en Ingeniería
Barcelona, Spain, April 6-10, 1992

NASA

Exponential Integration Algorithms Applied to Viscoplasticity

A. D. Freed
NASA Lewis Research Center
Cleveland, Ohio 44135

K. P. Walker
Engineering Science Software, Inc.
Smithfield, Rhode Island 02917

Abstract

Four, linear, exponential, integration algorithms (two implicit, one explicit and one predictor/corrector) are applied to a viscoplastic model to assess their capabilities. Viscoplasticity comprises a system of coupled, nonlinear, stiff, first order, ordinary differential equations which are a challenge to integrate by any means. Two of the algorithms (the predictor/corrector and one of the implicits) give outstanding results, even for very large time steps.

1 Nomenclature

C	is the creep strength.
D	is the drag strength.
h	is the nonlinear hardening parameter for yield strength.
H	is the hardening modulus for back stress.
L	is the limiting state for the dynamic recovery of back stress.
n	is the creep exponent.
Q	is the activation energy for creep (or self-diffusion).
r	is the thermal recovery parameter for yield strength.
R	is the universal gas constant, 8.314 J/mol-K.
t	is time, the dependent variable of the ODE.
T	is the absolute temperature.
T_0	is a reference temperature.
y	is the fraction of yield strength to applied stress at steady state.
Y	is the yield strength.
Z	is the Zener parameter.
B_{ij}	is the (deviatoric) back stress tensor.
$E_{ij} = \varepsilon_{ij} - \frac{1}{3}\varepsilon_{kk}\delta_{ij}$	is the deviatoric strain tensor.
$S_{ij} = \sigma_{ij} - \frac{1}{3}\sigma_{kk}\delta_{ij}$	is the deviatoric stress tensor.
U_α	is the linear coefficient of the ODE.
$\vec{V}_\alpha$	is the nonhomogeneous contribution to the ODE.
$\vec{X}_\alpha$	is the independent variable of the ODE.
α	is the coefficient of thermal expansion.

Δt	is an increment in time.
η	is the hardening modulus for yield strength.
ϑ	is the thermal diffusivity.
κ	is the bulk modulus.
μ	is the shear modulus.
δ_{ij}	is the Kronecker delta; 1 if $i = j$, otherwise 0.
ε_{ij}	is the infinitesimal strain tensor.
ε^p_{ij}	is the (deviatoric) plastic strain tensor.
σ_{ij}	is the Cauchy stress tensor.
$\Sigma_{ij} = S_{ij} - B_{ij}$	is the effective stress,
$\|\dot{\varepsilon}^p\| = \sqrt{2\dot{\varepsilon}^p_{ij}\dot{\varepsilon}^p_{ij}}$	is the magnitude of plastic strain rate.
$\|\Sigma\| = \sqrt{\frac{1}{2}\Sigma_{ij}\Sigma_{ij}}$	is the magnitude of effective stress.
$\langle x \rangle$	is the Macauley bracket of x; x if $x > 0$, otherwise 0.

2 Introduction

In many scientific fields, systems of first order, ordinary differential equations are used to model physical processes of interest. These equations are often coupled, mathematically stiff and/or nonlinear, thereby requiring special numerical algorithms for their solution [1]. Viscoplasticity is an example of such a modelling effort. The literature abounds with papers written on numerical integration methods applicable to viscoplasticity [2, 3, 4, 5, 6, 7], all of which testify to its complexity.

The paper begins with a presentation of four, linear, exponential, integration algorithms that have been recently derived by the authors [8]: two are implicit, the third is explicit, and the fourth is a predictor/corrector. The next section presents a viscoplastic model applicable to metals and solid solution alloys at high homologous temperatures. The final section presents numerical solutions for the viscoplastic model using the various integration algorithms. An appendix provides a discussion of Newton-Raphson iteration which we use in the solution schemes of the implicit integrators.

3 First Order ODEs

Viscoplasticity presents itself as a system of N (typically 3), coupled, nonlinear, stiff, first order, ordinary differential equations of the form

$$\dot{\vec{X}}_\alpha + U_\alpha \vec{X}_\alpha = \vec{V}_\alpha \qquad (\text{for } \alpha = 1, 2, \ldots, N), \tag{1}$$

where the $\vec{X}_\alpha[t]$ are the N independent scalar, vector or tensor variables to be solved for. The dot ' $\dot{}$ ' is used to denote differentiation with respect to time, t. The square brackets $[\cdot]$ are used to denote 'function of', while parentheses $(\cdot)$ and curly brackets $\{\cdot\}$ are used for mathematical groupings.

The parameters $U_\alpha\left[\vec{X}_\beta[t], t\right]$ and $\vec{V}_\alpha\left[\vec{X}_\beta[t], t\right]$ are, in general, functions of the variables $\vec{X}_\beta$ and t. If neither parameter is a function of the independent variables, then the system of equations is said to be linear; otherwise, it is nonlinear—as is the case in viscoplasticity. To simplify the notation, we use square brackets containing time to indicate the dependence of any variable on both $\vec{X}_\beta[t]$ and t. For example, we write $U_\alpha[t + \Delta t]$ and $\vec{V}_\alpha[t + \Delta t]$ to denote the values of the parameters $U_\alpha\left[\vec{X}_\beta[t + \Delta t], t + \Delta t\right]$ and $\vec{V}_\alpha\left[\vec{X}_\beta[t + \Delta t], t + \Delta t\right]$ at time $t + \Delta t$.

3.1 Two Implicit Algorithms

A technique like Newton-Raphson iteration (see the Appendix) must be used whenever a system of first order, ordinary differential equations is to be solved simultaneously using an implicit integration algorithm. We shall consider the following two implicit solutions for a system of N independent differential equations, *viz.* [8]

$$\vec{X}_\alpha[t+\Delta t] = \vec{X}_\alpha[t]\, e^{-U_\alpha[t+\Delta t]\cdot\Delta t} + \vec{V}_\alpha[t+\Delta t]\left(\frac{1-e^{-U_\alpha[t+\Delta t]\cdot\Delta t}}{U_\alpha[t+\Delta t]\cdot\Delta t}\right)\cdot\Delta t, \tag{2}$$

for $\alpha = 1, 2, \ldots, N$, and

$$\vec{X}_\alpha[t+\Delta t] = \vec{X}_\alpha[t]\, e^{-\frac{1}{2}(U_\alpha[t]+U_\alpha[t+\Delta t])\cdot\Delta t} + \tfrac{1}{2}\left(\vec{V}_\alpha[t]\, e^{-\frac{1}{2}(U_\alpha[t]+U_\alpha[t+\Delta t])\cdot\Delta t} + \vec{V}_\alpha[t+\Delta t]\right)\cdot\Delta t, \tag{3}$$

for $\alpha = 1, 2, \ldots, N$. These are the linear, asymptotic (2) and trapezoidal (3), implicit, exponential solutions for the integration of a system of ordinary differential equations (1). They are referred to as linear solutions becuase they were derived using Taylor and Euler-Maclaurin series expansions, respectively, that were truncated after their linear terms. Higher order (including exact) solutions can also be found in [8].

For large time steps, $\Delta t \gg 1$, with $U_\alpha > 0$, the exponential term becomes small compared with 1, and the asymptotic expansions

$$\lim_{\Delta t\to\text{large}} \vec{X}_\alpha[t+\Delta t] \asymp \frac{\vec{V}_\alpha[t+\Delta t]}{U_\alpha[t+\Delta t]} \tag{4}$$

and

$$\lim_{\Delta t\to\text{large}} \vec{X}_\alpha[t+\Delta t] \asymp \tfrac{1}{2}\vec{V}_\alpha[t+\Delta t]\cdot\Delta t \tag{5}$$

are obtained for the asymptotic (2) and trapezoidal (3) solutions, respectively. The asymptotic expansion given in (4) is the correct asymptotic solution for the first order differential equation (1). Hence, there is an advantage in using (2) over (3)—the asymptotic solution (2) is accurate and stable for time steps of all sizes for exponentially decaying solutions, like those which occur in viscoplasticity.

3.2 Explicit Algorithm

Different needs demand different solution techniques, and Newton-Raphson iteration will not always be the technique of choice. Newton-Raphson iteration is ideally suited for large computer codes where large time steps are needed to minimize the computation time. But it is not the best choice when small time steps are required for gaining a detailed picture of a response. For applications of this type, explicit solution techniques usually work best.

The linear, explicit, exponential, integration algorithm derived in [8] is given by

$$\vec{X}_\alpha[t+\Delta t] = \vec{X}_\alpha[t]\, e^{-U_\alpha[t]\cdot\Delta t} + \vec{V}_\alpha[t]\left(\frac{1-e^{-U_\alpha[t]\cdot\Delta t}}{U_\alpha[t]\cdot\Delta t}\right)\cdot\Delta t, \tag{6}$$

for $\alpha = 1, 2, \ldots, N$. Equation (6) differs from equation (2) in that all the terms on the right hand side of (6) are known explicitly; whereas, most of them in equation (2) are only known implicitly.

For large time steps, $\Delta t \gg 1$, with $U_\alpha > 0$, the exponential term becomes small compared with 1, and the asymptotic expansion

$$\lim_{\Delta t\to\text{large}} \vec{X}_\alpha[t+\Delta t] \asymp \frac{\vec{V}_\alpha[t]}{U_\alpha[t]} \tag{7}$$

is obtained for the explicit solution (6). Although the differences between the asymptotic (2) and explicit (6) solutions become negligible for small Δt, the differences between their asymptotic expansions, equations (4) and (7), can be enormous for large Δt. If we start at $t = 0$ and apply a large time increment Δt, the solution $\vec{V}_\alpha[\Delta t]/U_\alpha[\Delta t]$ for the implicit approximation is asymptotically correct, whilst that of the explicit solution, $\vec{V}_\alpha[0]/U_\alpha[0]$, corresponds to a ratio of the slopes of $\vec{V}_\alpha$ to U_α at the initial time, $t = 0$. In the case of viscoplasticity, these situations correspond to a correct viscoplastic solution in the implicit approximation, and an incorrect elastic solution in the explicit approximation, respectively. In subsequent time steps the explicit approximation will oscillate around the true solution, but it will not become unstable. These oscillations can be mitigated only by choosing smaller time steps.

3.3 Predictor/Corrector

Predictor/corrector methods use an explicit algorithm to first look ahead and *predict* the value of the function at a future point. Knowing something about the future response of this function, one then uses an implicit algorithm to go back and make a second, more accurate, *correction* of what the future value of this function is. These methods have the advantage of being able to use the difference between predicted $\vec{X}'_\alpha[t + \Delta t]$ and corrected $\vec{X}''_\alpha[t + \Delta t]$ values to establish an error which one can use to control the time step size, although that is not done herein.

A predictor/corrector based on linear exponential solutions [8] can be constructed by considering

$$\vec{X}'_\alpha[t + \Delta t] = \vec{X}_\alpha[t]\, e^{-U_\alpha[t]\cdot\Delta t} + \vec{V}_\alpha[t] \left(\frac{1 - e^{-U_\alpha[t]\cdot\Delta t}}{U_\alpha[t]\cdot\Delta t} \right) \cdot \Delta t \qquad (\text{for } \alpha = 1, 2, \ldots, N) \qquad (8)$$

for the predictor, and

$$\vec{X}''_\alpha[t + \Delta t] = \vec{X}_\alpha[t]\, e^{-U'_\alpha[t+\Delta t]\cdot\Delta t} + \vec{V}'_\alpha[t + \Delta t] \left(\frac{1 - e^{-U'_\alpha[t+\Delta t]\cdot\Delta t}}{U'_\alpha[t + \Delta t]\cdot\Delta t} \right) \cdot \Delta t \qquad (\text{for } \alpha = 1, 2, \ldots, N) \quad (9)$$

for the corrector, where

$$U'_\alpha[t + \Delta t] = U_\alpha\left[\vec{X}'_\beta[t + \Delta t], t + \Delta t\right] \qquad \text{and} \qquad \vec{V}'_\alpha[t + \Delta t] = \vec{V}_\alpha\left[\vec{X}'_\beta[t + \Delta t], t + \Delta t\right]. \qquad (10)$$

The predictor (8) is underdamped while the corrector (9) is overdamped; therefore, an improved estimate for updating the variable $\vec{X}_\alpha$ is obtained by averaging or weighting their values, *i.e.*

$$\vec{X}_\alpha[t + \Delta t] = \tfrac{1}{2} \left(\vec{X}'_\alpha[t + \Delta t] + \vec{X}''_\alpha[t + \Delta t] \right). \qquad (11)$$

In this integration algorithm, both the predictor and corrector are unconditionally stable, but the time step size must still be monitored for accuracy.

When considering either the asymptotic, explicit or predictor/corrector algorithm in the neighborhood of $U_\alpha \cdot \Delta t \approx 0$, one needs to expand $(1 - \exp[-U_\alpha \cdot \Delta t])/U_\alpha \cdot \Delta t$ into a power series in order to secure a sound computational algorithm.

These four, exponential, integration methods will now be applied to a viscoplastic model representative of copper at elevated temperatures.

4 Viscoplastic Model

Here we present a viscoplastic model where the governing system of differential equations is sufficiently complex to warrant a Jacobian of dimension greater than 1. Our implicit integration algorithms have an important advantage over classical algorithms—like backward Euler integration—in

that they have the distinct possibility of substantially reducting the order of the Jacobian. In this viscoplastic model there is a reduction in order from a 13×13 to a 2×2 for the Jacobian matrix (13 is the spatial dimension for this system of equations). This reduction in order is of importance from a computational viewpoint. For a more detailed discussion of viscoplasticity in general, see Lemaitre and Chaboche [9].

Viscoplastic constitutive models are currently finding application in describing the rate dependent plastic response of metallic structures that undergo significant temperature change over their duty cycle. The isotropic, stress/strain, constitutive equations are given by Hooke's law,

$$S_{ij} = 2\mu \left(E_{ij} - \varepsilon^p_{ij} \right) \qquad \text{with} \qquad \varepsilon^p_{kk} = 0, \tag{12}$$

$$\sigma_{kk} = 3\kappa \left\{ \varepsilon_{kk} - \alpha(T - T_0)\delta_{kk} \right\}, \tag{13}$$

where one sees that the plastic and thermal strains, ε^p_{ij} and $\alpha(T - T_0)\delta_{ij}$, are eigenstrains for the deviatoric and hydrostatic responses, respectively. The evolution of plastic strain is described by a flow law,

$$\dot{\varepsilon}^p_{ij} = \tfrac{1}{2} \|\dot{\boldsymbol{\epsilon}}^p\| \frac{\Sigma_{ij}}{\|\boldsymbol{\Sigma}\|}, \tag{14}$$

a kinetic law,

$$\|\dot{\boldsymbol{\epsilon}}^p\| = \vartheta[T]\, Z\left[\frac{\langle \|\boldsymbol{\Sigma}\| - Y \rangle}{D} \right], \tag{15}$$

and two evolutionary laws,

$$\dot{Y} = \eta \left(h[Y] \|\dot{\boldsymbol{\epsilon}}^p\| - r[T, Y] \right), \tag{16}$$

$$\dot{B}_{ij} = 2H \left(\dot{\varepsilon}^p_{ij} - \frac{B_{ij}}{2L[Y]} \|\dot{\boldsymbol{\epsilon}}^p\| \right). \tag{17}$$

Viscoplasticity is an internal state variable theory where the internal state variables, Y and B_{ij} in this case, are governed by separate evolution equations. The evolution of internal state follows a competitive process between hardening and recovery mechanisms (both thermal and dynamic). The yield strength Y is a phenomenological representation of material strength; it reflects the density of dislocations. The back stress B_{ij} is a phenomenological representation of an internal stress state; it reflects the stress fields set up by dislocations in their heterogeneous substructures.

We will consider a high-temperature viscoplastic model—valid for $T > \frac{1}{2} T_m$, where T_m is the absolute melting temperature—which is characterized by material functions that are power-laws; in particular:

$$\begin{aligned}
\vartheta[T] &= \exp\left[\frac{-Q}{RT} \right], \\
Z\left[\frac{\langle \|\boldsymbol{\Sigma}\| - Y \rangle}{D} \right] &= \left(\frac{\langle \|\boldsymbol{\Sigma}\| - Y \rangle}{D} \right)^3, \\
h[Y] &= \left(\frac{Y}{yC} \right)^{3-n}, \\
r[T, Y] &= \vartheta[T] \left(\frac{Y}{yC} \right)^3, \\
L[Y] &= \left(\frac{1}{y} - 1 \right) Y - D \left(\frac{Y}{yC} \right)^{n/3}.
\end{aligned} \tag{18}$$

Because of the chosen forms for the material functions h, L and r, this viscoplastic model *analytically* reduces to Odqvist's [10] classical theory of creep at steady state, where there is no evolution of the internal state variables, and where

$$\dot{\varepsilon}^p_{ij} = \tfrac{1}{2}\,\vartheta[T]\left(\frac{\|S\|}{C}\right)^n \frac{S_{ij}}{\|S\|} \tag{19}$$

defines the creep rate, with $\|S\| = \sqrt{\frac{1}{2}S_{ij}S_{ij}}$ characterizing the magnitude of deviatoric stress.

For illustrative purposes, we consider the material constants given in Table 1, which approximate copper behavior in the neighborhood of 500° Cin the absence of dynamic recrystallization.

5 Numerical Algorithms

If we differentiate equation (12), combine it with (14), and subtract (17) from both sides; and then rearrange equations (16) and (17), the following set of differential equations is obtained:

$$\dot{\Sigma}_{ij} + \frac{(\mu+H)\|\dot{\epsilon}^p\|}{\|\Sigma\|}\,\Sigma_{ij} \;=\; 2\mu\dot{E}_{ij} + \frac{H\|\dot{\epsilon}^p\|}{L[Y]}\,B_{ij}, \tag{20}$$

$$\dot{Y} + \eta\left(\frac{r[T,Y] - h[Y]\|\dot{\epsilon}^p\|}{Y}\right) Y \;=\; 0, \tag{21}$$

$$\dot{B}_{ij} + \frac{H\|\dot{\epsilon}^p\|}{L[Y]}\,B_{ij} \;=\; \frac{H\|\dot{\epsilon}^p\|}{\|\Sigma\|}\,\Sigma_{ij}. \tag{22}$$

This system of equations, $N = 3$, has the form of equation (1) where

$$\vec{X}_1 = \Sigma_{ij}, \qquad \vec{X}_2 = Y, \qquad \vec{X}_3 = B_{ij}, \tag{23}$$

$$U_1 = \frac{(\mu+H)\|\dot{\epsilon}^p\|}{\|\Sigma\|}, \qquad U_2 = \eta\left(\frac{r[T,Y] - h[Y]\|\dot{\epsilon}^p\|}{Y}\right), \qquad U_3 = \frac{H\|\dot{\epsilon}^p\|}{L[Y]}, \tag{24}$$

and

$$\vec{V}_1 = 2\mu\dot{E}_{ij} + \frac{H\|\dot{\epsilon}^p\|}{L[Y]}\,B_{ij}, \qquad \vec{V}_2 = 0, \qquad \vec{V}_3 = \frac{H\|\dot{\epsilon}^p\|}{\|\Sigma\|}\,\Sigma_{ij}. \tag{25}$$

These are the governing differential equations for our viscoplastic model when cast into the form of equation (1).

Upon examining equations (20–22), it becomes apparent why our Jacobian is at most a 3×3 matrix (one for each of the three differential equations), whereas the Jacobian for backward Euler integration is a 13×13 matrix (one for each of the thirteen spatial dimensions: six for the effective stress, six for the back stress, and one for the yield strength). However, our Jacobian must be further reduced to a 2×2 matrix. This is because U_1 and U_3 both become asymptotically proportional to $\|\dot{\epsilon}^p\|$ at steady state, and are therefore linearly dependent at steady state. Hence, either the evolution equation for back stress (22) or the evolution equation for effective stress (20) must not contribute to the construction of the Jacobian in order to prevent the Jacobian from becoming singular. Both approaches will work; however, they are not equivalent in computational efficiency. It is much more economical to construct the Jacobian matrix using equations (20 and 21) than using equations (21 and 22), because equation (20) contains information about the elastic response which is not present in equation (22).

5.1 Asymptotic Algorithm

The linear, implicit, asymptotic, exponential, integration algorithm, equation (2), can be written as

$$\vec{X}_\alpha[t+\Delta t] = \vec{X}_\alpha[t]\, e^{-\varrho_\alpha \cdot \Delta t} + \vec{V}_\alpha[t+\Delta t] \left(\frac{1 - e^{-\varrho_\alpha \cdot \Delta t}}{\varrho_\alpha \cdot \Delta t} \right) \Delta t \qquad \text{for} \qquad \alpha = 1,2 \tag{26}$$

where, for our viscoplastic model,

$$\varrho_1 = \frac{(\mu + H)\|\dot{\varepsilon}^p\|}{\|\boldsymbol{\Sigma}\|} \qquad \text{and} \qquad \varrho_2 = \eta \left(\frac{r[T,Y] - h[Y]\|\dot{\varepsilon}^p\|}{Y} \right), \tag{27}$$

which are both evaluated at time $t + \Delta t$. Thus, the iteration functions become

$$\mathcal{F}_1[\{\varrho_\beta\}_\lambda] = \frac{(\mu + H)\|\dot{\varepsilon}^p[\{\varrho_1, \varrho_2\}_\lambda]\|}{\|\boldsymbol{\Sigma}[\{\varrho_1\}_\lambda]\|} - \{\varrho_1\}_\lambda, \tag{28}$$

and

$$\mathcal{F}_2[\{\varrho_\beta\}_\lambda] = \frac{\eta \left(r\Big[T, Y[\{\varrho_2\}_\lambda]\Big] - h\Big[Y[\{\varrho_2\}_\lambda]\Big] \|\dot{\varepsilon}^p[\{\varrho_1, \varrho_2\}_\lambda]\| \right)}{Y[\{\varrho_2\}_\lambda]} - \{\varrho_2\}_\lambda, \tag{29}$$

which we have solved through Newton-Raphson iteration (*cf.* Appendix). The derivatives required to construct this 2×2 Jacobian matrix, *e.g.* $\partial\|\dot{\varepsilon}^p\|/\partial\varrho_1$, *etc.*, have been determined numerically, for in this case the determination of numerical derivatives is computationally more efficient than determining them analytically.

The Newton-Raphson iterations are accomplished by the following scheme. First, values of ϱ_1 and ϱ_2 are guessed. We set their values to 0.1 for the first time step, and used the converged values of the prior time step as the initial guess for all time steps thereafter. In addition, we also guess the values of Σ_{ij}, Y and B_{ij} in like manner. The forcing vectors, $\vec{V}_1$, $\vec{V}_2$ and $\vec{V}_3$ are then computed and used with ϱ_1 and ϱ_2 in the recursion relationships to determine $\vec{X}_1$, $\vec{X}_2$ and $\vec{X}_3$. Estimates of Σ_{ij}, Y and B_{ij} are now available to compute improved estimates of the forcing vectors, $\vec{V}_1$, $\vec{V}_2$ and $\vec{V}_3$ for the next iteration. It is evident from the preceding that this algorithm is basically one iteration in arrears in estimating Σ_{ij}, Y and B_{ij}.

The capability of this integration method is demonstrated in Fig. 1. The solid curve was obtained using 500 integration steps, and is considered to be the converged solution. In this example, a homogeneous block of material is sheared in a specified direction at a constant rate of straining to a fixed value of engineering strain, *i.e.* $\gamma \equiv 2\varepsilon_{12}$. This block of material is then sheared in the opposite direction to a self-similar value of engineering strain. The direction of loading is changed one last time to complete the loading cycle. The differences between the converged response and those determined using 25 and 3 integration steps are very small; however, there is a small amount of measurable error for the case of 10 integration steps at the knee of the curve.[1] These errors are enumerated in Table 2. At first glance, the fact that 3 integration steps do better than 10 seems contradictory. However the contradiction is apparent only, because the three integration points are close to their asymptotic solutions where the implicit, asymptotic, integration method is very accurate. The regions within which the 10 integration points are in greatest error are the transient domains where the back stress is rapidly evolving.

One important observation about this integration method is that the error generated in the transient domains does *not* propagate with the solution into the asymptotic domains. This is because the correct asymptotic solution (4) of the differential equation (1) is contained within the linear, implicit, asymptotic, integration method.

[1] For all of the results presented in this paper, none of the time steps were subincremented.

The increase in the shear stress from the first reversal to the final state is due to a gradual increase in the value of the yield strength Y over the loading history, *i.e.* the material is gradually getting stronger because of work hardening. The smooth curvature observed in the stress-strain response of each of the three loading segments is due to the rapid evolution of the back stress B_{ij} over each segment.

5.2 Trapezoidal Algorithm

For implicit, trapezoidal, Euler-Maclaurin integration, one can write the exponential solution (3) as

$$\vec{X}_\alpha[t+\Delta t] = \vec{X}_\alpha[t]\, e^{-\varrho_\alpha \cdot \Delta t} + \tfrac{1}{2}\left(\vec{V}_\alpha[t] e^{-\varrho_\alpha \cdot \Delta t} + \vec{V}_\alpha[t+\Delta t]\right)\cdot \Delta t \qquad \text{for} \qquad \alpha = 1,2 \tag{30}$$

where, for our viscoplastic model,

$$\varrho_1 = \frac{\mu + H}{2}\left(\frac{\|\dot{\varepsilon}^p[t]\|}{\|\Sigma[t]\|} + \frac{\|\dot{\varepsilon}^p[t+\Delta t]\|}{\|\Sigma[t+\Delta t]\|}\right), \tag{31}$$

and

$$\varrho_2 = \frac{\eta}{2}\left(\frac{r[t] - h[t]\|\dot{\varepsilon}^p[t]\|}{Y[t]} + \frac{r[t+\Delta t] - h[t+\Delta t]\|\dot{\varepsilon}^p[t+\Delta t]\|}{Y[t+\Delta t]}\right). \tag{32}$$

The associated iteration functions are therefore given by

$$\mathcal{F}_1\left[\{\varrho_\beta\}_\lambda\right] = \frac{\mu + H}{2}\left(\frac{\|\dot{\varepsilon}^p[t]\|}{\|\Sigma[t]\|} + \frac{\|\dot{\varepsilon}^p\left[\{\varrho_1, \varrho_2\}_\lambda\right]\|}{\|\Sigma\left[\{\varrho_1\}_\lambda\right]\|}\right) - \{\varrho_1\}_\lambda, \tag{33}$$

and

$$\begin{aligned}\mathcal{F}_2\left[\{\varrho_\beta\}_\lambda\right] \;=\; & \frac{\eta}{2}\left(\frac{r[t] - h[t]\|\dot{\varepsilon}^p[t]\|}{Y[t]} + \right. \\ & \left. + \;\frac{r\left[T, Y\left[\{\varrho_2\}_\lambda\right]\right] - h\left[Y\left[\{\varrho_2\}_\lambda\right]\right]\|\dot{\varepsilon}^p\left[\{\varrho_1, \varrho_2\}_\lambda\right]\|}{Y\left[\{\varrho_2\}_\lambda\right]}\right) - \{\varrho_2\}_\lambda,\end{aligned} \tag{34}$$

which are solved through Newton-Raphson iteration, as described in the Appendix.

The capability of this integration method is shown in Fig. 2 for the same loading history that was used in Fig. 1. The solid curve represents 500 integration points, and is equivalent to the converged response of Fig. 1, except at the locations of load reversal. The errors incurred by using fewer time steps, *viz.* 25, 10 and 3, are given in Table 2. Clearly one must monitor the size of the time step when using trapezoidal integration so as to secure accurate answers. Of the four, exponential, integration methods investigated herein for the numerical integration of viscoplastic models, the trapezoidal method is the least desirable. However for other applications, it can be the preferred method of integration [8].

It is apparent in Fig. 2 that the trapezoidal solution does not converge towards the asymptotic solution, as is the case with the asymptotic integration method. The inaccuracies attendant on the larger time steps are due to the representation in equation (20). The right hand side of this equation contains the term $\|\dot{\varepsilon}^p\|$ which depends in a highly nonlinear manner on the variable Σ_{ij} on the left hand side of the equation.

5.3 Explicit Algorithm

The linear, explicit, exponential, integration algorithm is much simpler than the prior two algorithms in that an iterative solution procedure is not required, and therefore there is no need to construct a Jacobian. The integration is effected by directly substituting the $\vec{X}$'s, U's and $\vec{V}$'s of equations (23–25) into the recursive solution (6).

The capability of this integration method is demonstrated in Fig. 3. Again, the solid curve represents the converged response. There is less error with this method than with the trapezoidal method for the larger time steps, as shown in Table 2. This is suprising at first glance because the trapezoidal method is implicit. The reason why the explicit algorithm does so well is that it contains the correct form for the asymptotic solution—the trapezoidal algorithm does not. Although the form of the asymptotic solution is correct, *i.e.* $\vec{V}_\alpha/U_\alpha$, it is evaluated at time t instead of time $t + \Delta t$, as it should be. As a consequence, several time steps must be incurred along the loading path to secure an accurate result, as observed in Fig. 3. If the time steps become too large the solution will oscillate, and the extent of oscillation will increase with the size of the time step.

For comparative purposes with Fig. 3, calculations obtained with the well-known forward Euler method are presented in Fig. 4. Our explicit method is the exponential analog of the forward Euler method. A comparison of errors between the explicit and forward Euler methods is also given in Table 2. It is apparent from both the figures and the table that the explicit exponential method is better than the explicit Euler method.

5.4 Predictor/Corrector

Like the explicit algorithm, the exponential predictor/corrector is simple to construct because a Jacobian is not required. The integration of the predictor follows the same logic as the explicit algorithm which was just discussed. With the predicted quantities $\vec{X}'_\alpha[t + \Delta t]$ now known, the U's and $\vec{V}$'s are updated to time $t + \Delta t$, and integration via the corrector is effected by substituting equations (23–25) into the recursive implicit solution (9). For the results presented herein, the predictor and corrector were both integrated once at each time step—there was no iteration of the corrector.

The ability of this integration method is demonstrated in Figs. 5 and 6. As before, the solid curves represent the converged solution and were obtained using 500 integration steps. In Fig. 5, the results that are presented are the corrected (not weighted) values $\vec{X}''$ coming from equation (9). In Fig. 6, the results that are presented are the averaged (weighted) values $\frac{1}{2}(\vec{X}' + \vec{X}'')$ coming from equation (11). In both cases, the presence of the corrector dampens the oscillations that are present in the explicit (predictor) solution, *cf.* Fig. 3. The reason why an improved result is obtained by averaging the predicted and corrected values is because the predictor is underdamped while the corrector is overdamped. Consequently, averaging them tends to remove much of the unwanted damping.

For comparative purposes with our weighted predictor/corrector, *i.e.* Fig. 6, calculations obtained with the well-known Heun method are presented in Fig. 7. A comparison of errors between these two methods is also given in Table 2. The weighted predictor/corrector is the exponential analog of Heun's method, which is a second order Runge-Kutta method. It is apparent from both the figures and the table that the exponential, weighted, predictor/corrector is better than the Heun method.

6 Concluding Remarks

Four, linear, exponential, integration algorithms that we derived in [8] have been applied to a viscoplastic model which is composed of a system of coupled, nonlinear, stiff, first order, ordinary differential equations. Of these four methods, two have been found to have superior properties for the solution of these equations. The implicit asymptotic algorithm is the most accurate, but it requires the construction of a Jacobian matrix. It is recommended for large computer codes like finite elements. The averaged or weighted predictor/corrector also has exceptional accuracy, plus it has the advantage of not needing a Jacobian. It is recommended for smaller codes, and for those cases when implicit algorithms are not practical, *e.g.* our composite micromechanics theory [11].

For exponentially decaying solutions, like those which occur in viscoplasticity, these two integration algorithms have the following desirable properties:

- They are asymptotically correct.
- They are stable and accurate for both small and large time steps.
- They do not propagate error.
- They are computationally efficient.

When compared with equivalent classical methods, the exponential integration algorithms are superior. This is because viscoplasticity has exponential solutions for which the exponential integration algorithms are better suited.

Acknowledgment

This work (for K.P.W.) was supported by the NASA Lewis Research Center under Grant NAG3-1258, and by the Department of Energy under Contract DE-AC02-88ER13895.

References

[1] C.W. GEAR, *Numerical Initial Value Problems in Ordinary Differential Equations,* (Prentice-Hall, Englewood Cliffs, NJ, 1969).

[2] R.D. KRIEG, "Numerical Integration of Some New Unified Plasticity-Creep Formulations," in 4th International Conference on Structural Mechanics in Reactor Technology, (SMIRT IV, San Francisco, 1977), paper M 6/4.

[3] V. BANTHIA AND S. MUKHERJEE, "On an Improved Time Integration Scheme for Stiff Constitutive Models of Inelastic Deformation," *J. Eng. Mater. Technol.*, **107**, 282–285 (1985).

[4] T.G. TANAKA AND A.K. MILLER, "Development of a Method for Integrating Time-Dependent Constitutive Equations With Large, Small or Negative Strain Rate Sensitivity," *Int. J. Num. Meth. Eng.*, **26**, 2457–2485 (1988).

[5] A.M. LUSH, G. WEBER, AND L. ANAND, "An Implicit Time-Integration Procedure for a Set of Internal Variable Constitutive Equations for Isotropic Elasto-Viscoplasticity," *Int. J. Plast.*, **5**, 521–549 (1989).

[6] A. BENALLAL, P. CHABRAND, M. GHAZOUANE, M. CHAUDONNERET, J.P. CULIÉ, E. CONTESTI, H. GAMHA, J.C. GOLINVAL, AND A. TURBAT, "Validation of Structural Computation Codes in Elastoviscoplasticity," *Int. J. Num. Meth. Eng.*, **29**, 1109–1130 (1990).

[7] J.W. Ju, "Consistent Tangent Moduli for a Class of Viscoplasticity," *J. Eng. Mech.*, **116**, 1764–1779 (1990).

[8] K.P. Walker and A.D. Freed, *Asymptotic Integration Algorithms for Nonhomogenous, Nonlinear, First Order, Ordinary Differential Equations,* (NASA TM–103793, 1991). Submitted to *J. Comp. Phys.*

[9] J. Lemaitre and J-L. Chaboche, *Mechanics of Solid Materials,* (Cambridge University Press, London, 1990), ch. 6.

[10] F.K.G. Odqvist, *Mathematical Theory of Creep and Creep Rupture,* 2nd ed. (Oxford University Press, London, 1974), ch. 5.

[11] K.P. Walker, E.H. Jordan, and A.D. Freed, *Nonlinear Mesomechanics of Composites With Periodic Microstructure: First Report,* (NASA–TM 102051, 1989).

Appendix: Newton-Raphson Iteration

In general the ϱ_α, where $\varrho_\alpha = U_\alpha[t+\Delta t]$ in (2) or $\varrho_\alpha = \frac{1}{2}\left(U_\alpha[t] + U_\alpha[t+\Delta t]\right)$ in (3), are functions of the $\vec{X}_\beta[t+\Delta t]$ which are in turn, *via* (2) or (3), functions of the $\varrho_\nu[t+\Delta t]$, and therefore

$$\varrho_\alpha\left[\vec{X}_\beta\left[\varrho_\nu\right]\right] = \mathcal{G}_\alpha\left[\varrho_\nu\right] \qquad (\text{for } \alpha,\beta,\nu = 1 \text{ to } N), \tag{A1}$$

or equivalently,

$$\mathcal{F}_\alpha\left[\varrho_\nu\right] = 0, \tag{A2}$$

where

$$\mathcal{F}_\alpha\left[\varrho_\nu\right] \equiv \mathcal{G}_\alpha\left[\varrho_\nu\right] - \varrho_\alpha. \tag{A3}$$

If $\{\varrho_\alpha\}_\lambda$ is the λ^{th} guess for vector ϱ_α, then the true solution satisfying (2) or (3) may be written as

$$\varrho_\alpha = \{\varrho_\alpha\}_\lambda + c_\alpha, \tag{A4}$$

where the correction vector, c_α, is the amount by which the true vector differs from the guessed value. Inserting this definition into (A2), and expanding the resultant by Taylor's theorem while retaining only the first order terms leads to

$$\mathcal{F}_\alpha[\varrho_\nu] \;=\; \mathcal{F}_\alpha\left[\{\varrho_\nu\}_\lambda + c_\nu\right] \;\simeq\; \mathcal{F}_\alpha\left[\{\varrho_\nu\}_\lambda\right] + \sum_{\beta=1}^{N} \frac{\partial \mathcal{F}_\alpha[\{\varrho_\nu\}_\lambda]}{\partial\{\varrho_\beta\}_\lambda}\, c_\beta \;=\; 0. \tag{A5}$$

A solution to the resulting linear system of equations,

$$\sum_{\beta=1}^{N} J_{\alpha\beta}\, c_\beta = -\mathcal{F}_\alpha[\{\varrho_\nu\}_\lambda] \qquad (\text{for } \alpha = 1 \text{ to } N), \tag{A6}$$

for the unknown correction vector, c_β, with Jacobian,

$$J_{\alpha\beta} = \frac{\partial \mathcal{F}_\alpha[\{\varrho_\nu\}_\lambda]}{\partial\{\varrho_\beta\}_\lambda}, \tag{A7}$$

can be obtained by Cramer's rule ($N \leq 3$) or Gaussian elimination ($N \geq 4$). This leads to an improved value for the solution vector, $\{\varrho_\alpha\}_{\lambda+1}$, where

$$\{\varrho_\alpha\}_{\lambda+1} = \{\varrho_\alpha\}_\lambda + c_\alpha, \tag{A8}$$

which is iterated until the contribution from c_α becomes negligible (we used $\|c\| < 0.0001\|\varrho\|_\lambda$ as our convergence criterion).

In order to retain algorithmic stability, it is necessary to bound the size of the correction vector so that

$$\|c\| \leq \Upsilon \, \|\varrho\|_\lambda \tag{A9}$$

(we typically set $\Upsilon \approx 0.1$) where

$$\|c\| = \sqrt{{c_1}^2 + {c_2}^2 + \cdots + {c_N}^2} \qquad \text{and} \qquad \|\varrho\|_\lambda = \sqrt{\{\varrho_1\}_\lambda^2 + \{\varrho_2\}_\lambda^2 + \cdots + \{\varrho_N\}_\lambda^2} \, . \tag{A10}$$

That is, if

$$\|c\| > \Upsilon \, \|\varrho\| \qquad \text{set} \qquad c_\alpha \Rightarrow c_\alpha \frac{\Upsilon \, \|\varrho\|_\lambda}{\|c\|} \qquad \forall \, \alpha \in \{1, N\} \tag{A11}$$

in equation (A8). This slows down the rate of convergence, but it keeps the procedure stable and free of oscillations. What we are actually doing is keeping the solution within the domain of applicability of the truncated Taylor expansion given in equation (A5).

If possible, the Jacobian (A7) should be determined analytically; if not, it can be acquired numerically, but often times at a greater numerical expense. Because Newton-Raphson iteration has quadratic convergence, the number of iterations λ required for convergence is usually few in number. One reasonable initial guess to advance the iteration process to the next step is to use the values from the last time step, *i.e.* set $\varrho_\alpha[t + \Delta t]_{\lambda=1} = \varrho_\alpha[t]$.

Table 1: Elastic and viscoplastic material constants.

Constant	Units	Value
α	$1/^\circ$ C	20×10^{-6}
κ	MPa	95,000
μ	MPa	30,000
C	MPa	0.8
D	MPa	0.016
H	MPa	15,000
n	—	5
Q	J/mol.	200,000
y	—	0.1
η	MPa	30,000

Table 2: Percent error in the range of stress, $100 \cdot |(\sigma - \sigma_{500})/\sigma_{\max}|$, evaluated at two points in the third branch of each curve. Errors greater than 100% are denoted as > 100. There the algorithm is outside its domain of applicability and the error is meaningless.

Algorithm Type	Integration Points				
	$\varepsilon = 0.0$		$\varepsilon = 0.005$		
	10	25	3	10	25
Asymptotic	9.8	2.1	1.8	1.2	0.3
Trapezoidal	26.2	2.3	>100	38.7	6.2
Explicit	19.6	0.9	56.5	12.5	0.0
Forward Euler	17.3	19.8	>100	>100	1.5
Predictor/Corrector	23.9	5.0	>100	16.1	0.7
Weighted Pred/Corr	1.3	0.0	45.3	0.6	0.3
Heun	62.0	15.8	>100	26.0	1.6

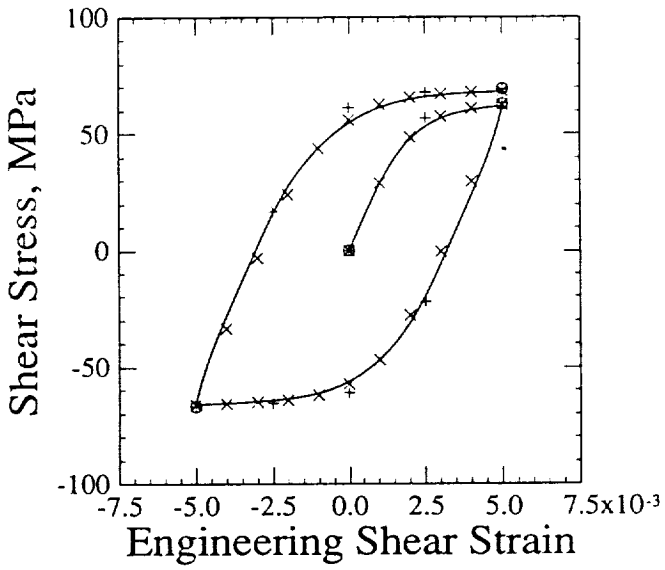

Figure 1.—Linear, implicit, asymptotic solutions for the viscoplastic representation of copper. $\dot{\gamma} = \pm 0.001 s^{-1}$. T = 500 °C. $Y|_{t=0}$ = 1 MPa. The integration points were evenly spaced: — represents 500 steps, x represents 25 steps, + represents 10 steps, and o represents 3 steps.

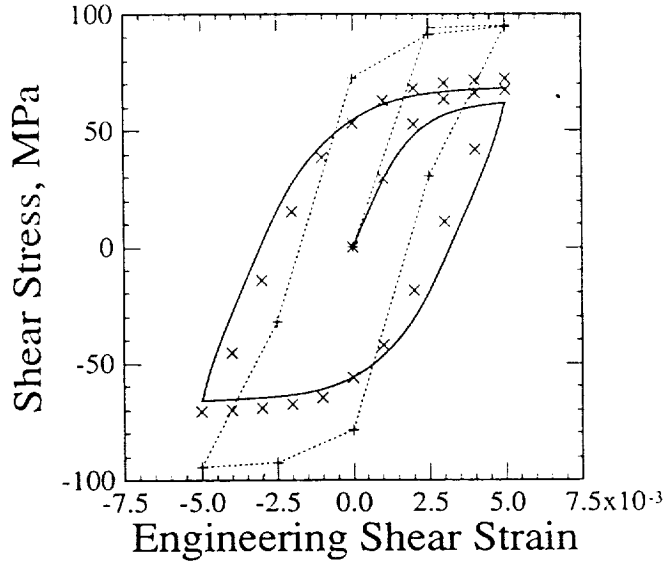

Figure 2.—Trapezoidal Euler-Maclaurin solutions for the viscoplastic representation of copper. $\dot{\gamma} = \pm 0.001 s^{-1}$. T = 500 °C. $Y|_{t=0}$ = 1 MPa. The integration points were evenly spaced: — represents 500 steps, x represents 25 steps, and + represents 10 steps. Stresses for 3 integration steps exceeded the plotted range of stress.

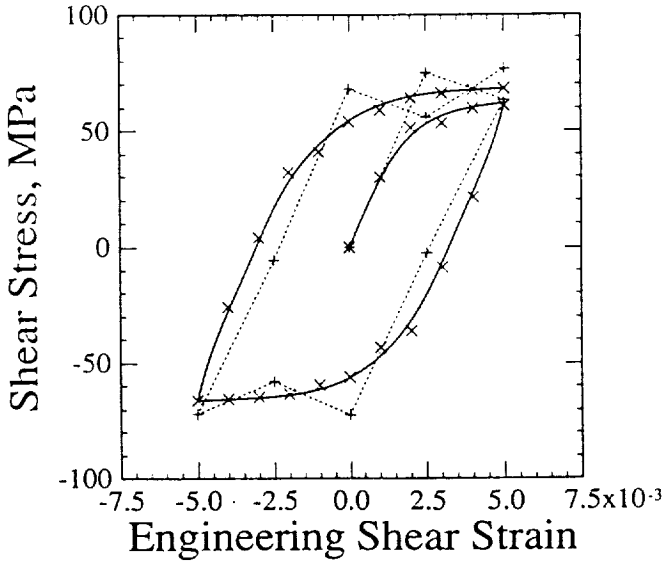

Figure 3.—Linear explicit solutions for the viscoplastic representation of copper. $\dot{\gamma} = \pm 0.001 s^{-1}$. T = 500 °C. $Y|_{t=0}$ = 1 MPa. The integration points were evenly spaced: — represents 500 steps, x represents 25 steps, and + represents 10 steps. Stresses for 3 integration steps exceeded the plotted range of stress.

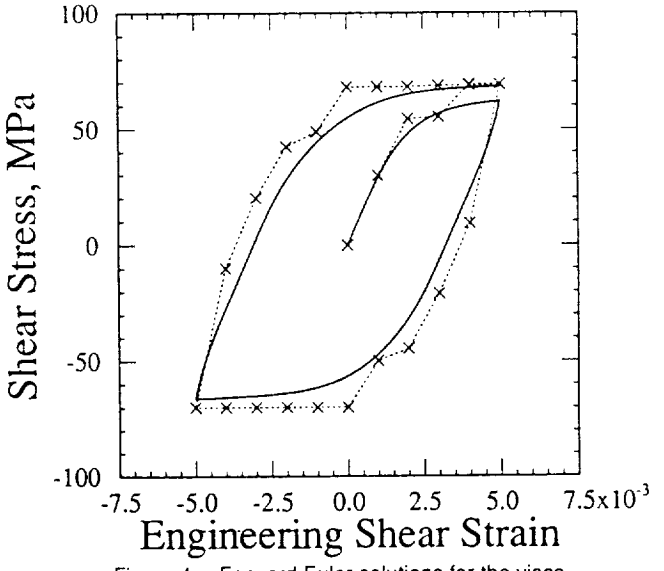

Figure 4.—Forward Euler solutions for the viscoplastic representation of copper. $\dot{\gamma} = \pm 0.001 s^{-1}$. T = 500 °C. $Y|_{t=0}$ = 1 MPa. The integration points were evenly spaced: — represents 500 steps and x represents 25 steps. Stresses for 10 and 3 integration steps exceeded the plotted range of stress.

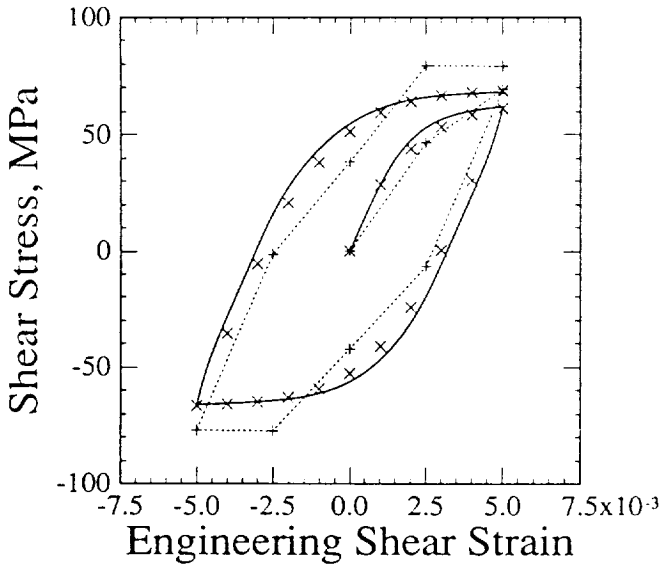

Figure 5.—Linear predictor/corrector solutions (not weighted) for the viscoplastic representation of copper. $\dot{\gamma} = \pm 0.001 s^{-1}$. T = 500 °C. $Y|_{t=0}$ = 1 MPa. The integration points were evenly spaced. —— represents 500 steps, x represents 25 steps, and + represents 10 steps. Stresses for 3 integration steps exceeded the plotted range of stress.

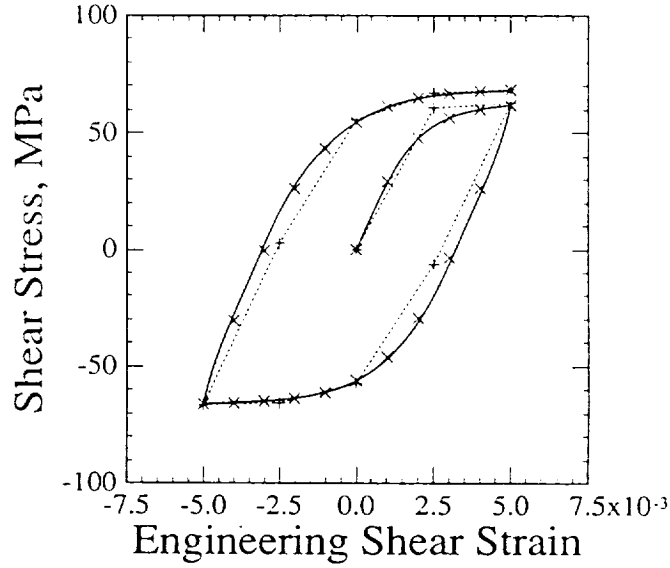

Figure 6.—Linear predictor/corrector solutions (weighted) for the viscoplastic representation of copper. $\dot{\gamma} = \pm 0.001 s^{-1}$. T =500 °C. $Y|_{t=0}$ = 1 MPa. The integration points were evenly spaced. —— represents 500 steps, x represents 25 steps, and + represents 10 steps. Stresses for 3 integration steps exceeded the plotted range of stress.

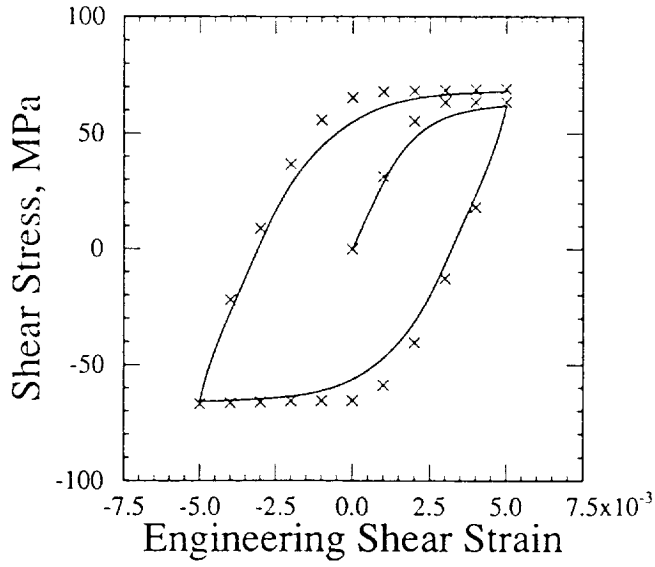

Figure 7.—Heun (a second order Runge-Kutta) solutions for the viscoplastic representation of copper. $\dot{\gamma} = \pm 0.001 s^{-1}$. T = 500 °C. $Y|_{t=0}$ = 1 MPa. The integration points were evenly spaced. —— represents 500 steps and x represents 25 steps. Stresses for the 10 and 3 integration steps exceeded the plotted range of stress.

NASA
National Aeronautics and Space Administration

Report Documentation Page

1. Report No.	2. Government Accession No.	3. Recipient's Catalog No.
NASA TM-104461		

4. Title and Subtitle	5. Report Date
Exponential Integration Algorithms Applied to Viscoplasticity	
	6. Performing Organization Code

7. Author(s)	8. Performing Organization Report No.
A.D. Freed and K.P. Walker	E-6302
	10. Work Unit No. 553-13-00

9. Performing Organization Name and Address	11. Contract or Grant No.
National Aeronautics and Space Administration Lewis Research Center Cleveland, Ohio 44135-3191	
	13. Type of Report and Period Covered Technical Memorandum
12. Sponsoring Agency Name and Address	14. Sponsoring Agency Code
National Aeronautics and Space Administration Washington, D.C. 20546-0001	

15. Supplementary Notes

Prepared for the Third International Conference on Computational Plasticity Fundamentals and Applications (COMPLAS III) sponsored by the Centro Internacional de Métodos Numéricos en Ingeniería, Barcelona, Spain, April 6-10, 1992. A.D. Freed, NASA Lewis Research Center; K.P. Walker, Engineering Science Software, Inc., Smithfield, Rhode Island 02917. Responsible person, A.D. Freed, (216) 433-3262.

16. Abstract

Four, linear, exponential, integration algorithms (two implicit, one explicit and one predictor/corrector) are applied to a viscoplastic model to assess their capabilities. Viscoplasticity comprises a system of coupled, nonlinear, stiff, first order, ordinary differential equations which are a challenge to integrate by any means. Two of the algorithms (the predictor/corrector and one of the implicits) give outstanding results, even for very large time steps.

17. Key Words (Suggested by Author(s))	18. Distribution Statement
Numerical integration Differential equations Viscoplasticity	Unclassified - Unlimited Subject Category 64

19. Security Classif. (of the report)	20. Security Classif. (of this page)	21. No. of pages	22. Price*
Unclassified	Unclassified	16	A03

NASA FORM 1626 OCT 86

*For sale by the National Technical Information Service, Springfield, Virginia 22161